

Electron-Ion Equilibration in Ultrafast Heated Graphite

T. G. White,^{1,*} N. J. Hartley,¹ B. Borm,² B. J. B. Crowley,^{1,3} J. W. O. Harris,³ D. C. Hochhaus,⁴ T. Kaempfer,⁵
K. Li,⁴ P. Neumayer,⁴ L. K. Pattison,³ F. Pfeifer,² S. Richardson,^{1,3} A. P. L. Robinson,⁶
I. Uschmann,⁵ and G. Gregori^{1,†}

¹*Department of Physics, University of Oxford, Parks Road, Oxford OX1 3PU, United Kingdom*

²*Goethe-Universität, D-60438 Frankfurt am Main, Germany*

³*AWE, Aldermaston, Reading, Berkshire RG7 4PR, United Kingdom*

⁴*ExtreMe Matter Institute EMMI and Research Division, GSI Helmholtzzentrum für Schwerionenforschung, 64291 Darmstadt, Germany*

⁵*Helmholtzinstitut Jena, Fröbelstieg 1, D-07743 Jena, Germany*

⁶*Central Laser Facility, STFC Rutherford Appleton Laboratory, Oxfordshire OX11 0QX, United Kingdom*

(Received 14 October 2013; published 10 April 2014)

We have employed fast electrons produced by intense laser illumination to isochorically heat thermal electrons in solid density carbon to temperatures of $\sim 10\,000$ K. Using time-resolved x-ray diffraction, the temperature evolution of the lattice ions is obtained through the Debye-Waller effect, and this directly relates to the electron-ion equilibration rate. This is shown to be considerably lower than predicted from ideal plasma models. We attribute this to strong ion coupling screening the electron-ion interaction.

DOI: [10.1103/PhysRevLett.112.145005](https://doi.org/10.1103/PhysRevLett.112.145005)

PACS numbers: 52.50.Gj, 05.70.Ln, 61.05.cp, 81.05.uf

Solid density carbon with pressures above one megabar and temperatures in the thousands of kelvin lie in the warm dense matter (WDM) region, which sits between the traditional solid state and the high-temperature plasma domains. Expansion techniques are no longer applicable and neither the kinetic nor the potential energy can be treated perturbatively; as such, the phase diagram of carbon is still largely unknown for both the highly excited solid [1] and fluid phases [2]. These extreme matter states are highly relevant to the understanding of the evolution and the structure of large planets and compact objects [3–7], as well as for inertial confinement fusion experiments [8,9], equation of state, and opacity models [10].

WDM states are created in the laboratory using lasers or pulsed power machines [11] and result in a system of highly coupled ionic liquids immersed in a partially degenerate electron sea. On short time scales, due to the preferential and rapid heating of one subsystem (electrons or ions, depending on the details of the excitation mechanism) over the other, there is no guarantee that the matter will be in thermodynamic equilibrium. Indeed, such is the rate of heating that a nonequilibrium theory of plasmas would be best suited for analysis, although the rapid equilibration within the subsystems means two-temperature models are a viable approach [12]. Relatively few experiments have attempted to measure relaxation rates [13–16], and they seem to indicate relaxation times that are much longer than those predicted by ideal or nearly ideal plasma models [17,18]. This behavior, which essentially suggests a weak energy coupling between electrons and ions, has been attributed to the excitation of collective modes that screen

the electron-ion potential, and thus reduce the energy transfer [19–22]. Depending on the exact implementation of such coupled-mode theories, relaxation times between 1 and 2 orders of magnitude smaller than that produced by the ideal Spitzer-Brysk model [17,18] have been predicted. Experimental verification is thus essential, and, at the same time, knowledge of the times over which the energy relaxation processes occur is of fundamental importance in any WDM work.

Here we focus our work on graphite, which has the highest electron mobility and thermal conductivity of any bulk material, and displays unique electronic [23] and phonon properties [26]. It also exhibits exceptionally low relaxation rates [16,24,26–32] that disagree with current theoretical models [27]. However, in the interpretation of the experimental data, uncertainties remain in disentangling the excitation mechanism with the relaxation pathways. While the overall energy transfer between electrons and ions is slow, a strong interaction between the excited electrons and high energy (~ 200 meV) coupled optical phonons can still occur [26]. Although previous experiments have investigated lattice temperature in weakly to moderately driven systems (e.g., [16,24,25]) these utilized different methods of heating, with either direct coupling of a pump laser to optical phonons (see, e.g., Ref. [26]) or a high energy proton beam [16]. Here we present the results of an experiment where a graphite sample has been heated to very high temperatures by a fast electron beam, but preserving the initial lattice structure. This allows us to investigate electron-phonon coupling in the high-temperature limit, that is, near melting. Energy deposition by fast

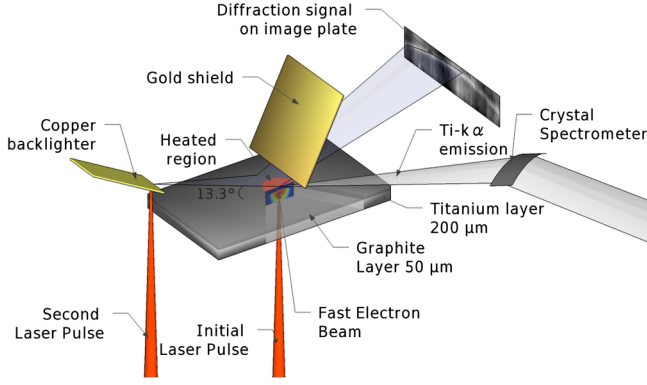


FIG. 1 (color online). Schematic of the experimental setup. The experiment was performed at the PHELIX Laser Facility, GSI Helmholtz Facility, Germany. The 80 J, 0.7 ps beam at the fundamental wavelength $\lambda_0 = 1054$ nm was split into two arms in a pump-probe configuration. To heat the graphite sample, 50% of the energy was delivered onto the titanium substrate with a $30 \mu\text{m}$ focal spot. The fast electron distribution heats the graphite attached to the rear of the sample. The remaining energy was focused between 0 and 1000 ps later with a $30 \mu\text{m}$ focal spot onto a copper foil to generate Cu-K α probe x rays. The copper foil is angled with respect to the target to reduce the source size. An image plate detector was placed 100 mm away from the graphite sample at 13.3° to detect the Bragg diffracted light.

electrons also avoids many issues related to laser heating of solids, e.g., direct coupling of the laser light to phonon modes and inhomogeneous heating. Moreover, electron heating occurs on times shorter than in the case of proton driven samples, and the stopping power is very different in the two cases.

The experiment was carried out at the PHELIX Laser Facility at the GSI Helmholtz Institute (Darmstadt, Germany). Figure 1 shows the schematic of the experiment. A 0.7 ps long laser pulse delivering 80 J of energy was split into two equal arms, with one focused onto a $200 \mu\text{m}$ thick Ti substrate with the rear surface coated with a $50 \mu\text{m}$ thick highly orientated pyrolytic graphite layer. The presence of the Ti substrate enables the electrons to isochorically heat the graphite while preventing direct illumination from the laser. The interaction drives a nonthermal fast electron current through the target. These electrons are accelerated by the radiation field of the laser pulse and can reach energies of the order of 1 keV to several MeV [33]. The background thermal electrons in the solid target respond to this fast electron current by setting up resistive electric fields and strong return currents. Through a process of collisions and Ohmic heating, the fast electron population loses energy to the surrounding material.

The high energy electrons that are accelerated through the solid target also produce intense x-ray and vacuum ultraviolet emission, primarily through bremsstrahlung radiation and K-shell ionization. The resulting Ti K-shell line emission was collected with an absolutely calibrated,

toroidally bent spectrometer [34,35] and used to infer the single shot properties (spectral temperature, angular divergence, and absorbed laser energy) of the fast electron population [36–38].

The second laser beam is delayed by a varying amount (0–1000 ps) with respect to the first and irradiates a copper foil acting as a short pulse source of 8 keV Cu-K α line radiation (see Fig. 1). The x rays diffract off the graphite layer at a Bragg angle of 13.3° onto an image plate detector placed 100 mm away. The magnification of the setup was 38. The copper foil is tilted edge-on with respect to the sample in order to reduce source broadening. The temperature of the graphite ions is related to the intensity of the Bragg scattered x rays via the Debye-Waller effect:

$$I = \exp \left[-\frac{6k^2\hbar^2}{Mk_B T_D} \left(\frac{T_i^2}{T_D^2} \int_0^{T_D/T_i} \frac{udu}{e^u - 1} + \frac{1}{4} \right) \right], \quad (1)$$

where T_i is the ion temperature, M is ion mass, T_D the Debye temperature, and k the scattering wave vector. This relation shows that there is a reduction in the scattered intensity due to increased thermal vibrations of the atoms around their equilibrium lattice sites [39]. A value of $T_D = 800$ K was extracted from density functional theory calculations and shown to have little variation with electron temperatures in the range considered in our experiment [16]. Figure 2 shows the decrease in the measured intensity of the scattered x rays across the surface of the graphite sample for two different time delays. As the electrons transfer their energy to the ions, the ion temperature increases, and a more pronounced reduction in the diffracted intensity becomes apparent in the data.

The experimental data showing the increase in ion temperature over time can be fitted with a simple two-temperature model:

$$C_e \frac{\partial T_e}{\partial t} = \nabla(K_e \nabla T_e) - g(T_e - T_i) + S_e \delta(t), \quad (2a)$$

$$C_i \frac{\partial T_i}{\partial t} = \nabla(K_i \nabla T_i) + g(T_e - T_i), \quad (2b)$$

where C_e (C_i) is the electron (ion) specific heat capacity, K_e (K_i) is the electron (ion) thermal conductivity, and S_e is the Ohmic heating term due to the return current. Here we assume that heating occurs over a much shorter time (of the order of the laser pulse duration, 0.7 ps) than the time scale for electron-ion equilibration. This also agrees with a resistive skin time of ~ 1 ps across $50 \mu\text{m}$ graphite. The temperature-dependent heat capacities of the electrons and ions were obtained from density functional theory calculations [2,16]. The thermal conductivity term can be neglected in this case as thermal diffusion occurs on a microsecond time scale and radiative transport is negligible at these temperatures (see the Supplemental Material [40]).

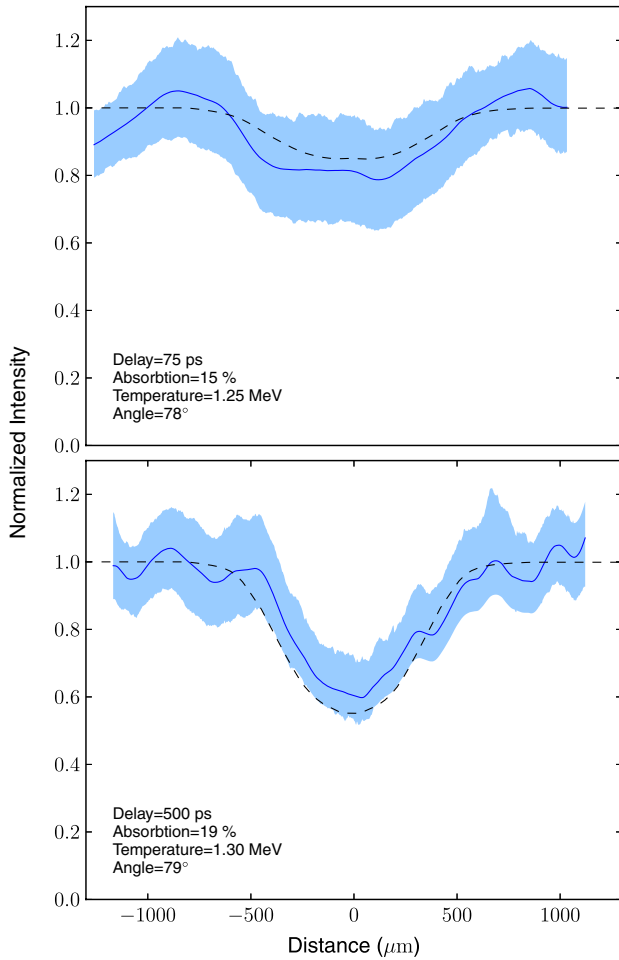


FIG. 2 (color online). Experimental data showing the reduction in intensity of Bragg scattering from the surface of the graphite (solid lines) for two different delays of 75 and 500 ps. Experimental error bars are represented by the shaded region. The dashed line shows simulation results taken from the ZEPHYROS fast electron code applied to the two-temperature model with a coupling constant of $0.2 \times 10^{16} \text{ W K}^{-1} \text{ m}^{-3}$. Also shown are the calculated absorption, temperature, and divergence angle of the fast electron distribution through comparison with the emitted Ti K -shell line emission.

The transfer rate is set by the coupling constant g . This method allows the complexity of the physical system to be contained within a single parameter. The coupling constant is a quantity that is difficult to estimate from first principles as it depends on the interaction dynamics of the electron and phonon subsystems. Within the two temperature model, g and S_e are chosen as fitting parameters such that the predicted ion temperature in the graphite sample reproduces the measured reduction in the Bragg peak intensity. The best fit, by matching the ion temperature at the center of the heated region, is found to be a coupling constant of $g = (0.15\text{--}0.25) \times 10^{16} \text{ W K}^{-1} \text{ m}^{-3}$ and a source energy density of $S_e = 6\text{--}8 \text{ J mm}^{-3}$, as shown in Fig. 3.

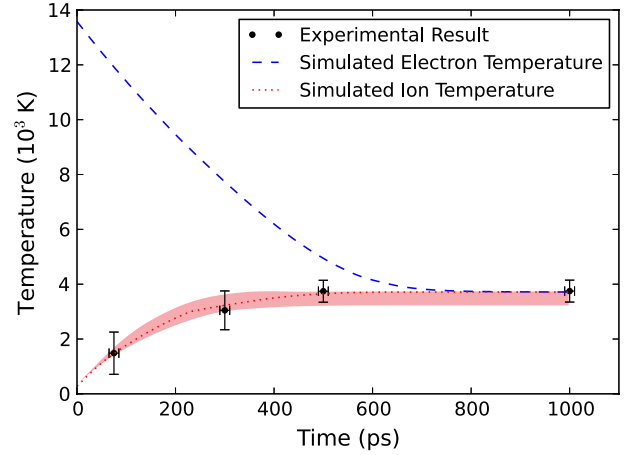


FIG. 3 (color online). Time evolution of the electron (blue dashed line) and ion (red dotted line) temperatures using a coupling constant $g = 0.2 \times 10^{16} \text{ W K}^{-1} \text{ m}^{-3}$ and source term $S_e = 7 \text{ J mm}^{-3}$. The points represent the experimentally measured ion temperature. The shaded region represents varying the source term from 6 to 8 J mm^{-3} .

In addition to fitting the two-temperature model to the experimental ion temperature, the source term can be calculated from the Ti K -shell emission. This was achieved by modeling the energy deposition throughout the sample using the 3D hybrid code ZEPHYROS [41]. Here, the fast electrons are treated as macroparticles as in a typical particle-in-cell code, while the background electrons and ions are modeled as a fluid. The resistivity is handled within a reduced Lee-Moore model [42] and matches published values for room-temperature graphite [43,44]. ZEPHYROS also includes a K -shell photon emission rate [45]. In this way, the initial fast electron population is varied until the predicted K -shell emission from the simulation matches the experimental result (see Fig. 4 for details). It has been shown that the absorbed energy, spectral temperature, and divergence angle can be uniquely identified using this method [36]. The source term for the two-temperature model found through this method is $S_e = 6.9 \text{ J mm}^{-3}$, which is in agreement with the value found through fitting the data. With this spatially dependent source term from ZEPHYROS, we can plot the predicted intensity drop across the back surface at different times after heating; see Fig. 2. We find good agreement between simulation and experiment for a coupling constant $g = 0.2 \times 10^{16} \text{ W K}^{-1} \text{ m}^{-3}$.

Because of the complexities associated with short pulse laser irradiation and fast electron transport, the assumption that the heating is uniform and instantaneous should be discussed. The intense fast electron current in the target produces large magnetic and electric fields that can complicate the analysis through magnetic focusing, the formation of resistive current loops, and large-scale instabilities arising from a varying resistance with temperature

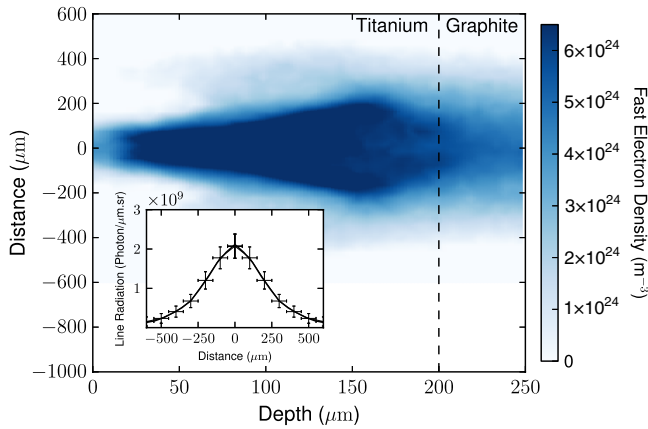


FIG. 4 (color online). Simulation results from the ZEPHYROS electron transport code. The fast electron density (units $1/m^3$) is shown at $t = 0.8$ ps. The inset shows the Ti-K α emission from the simulation and the experimental measurement using an absolutely calibrated imaging spectrometer. The fit has a p value > 0.999 .

[46,47]. As shown in the Supplemental Material [40], these effects remain small in our experiment, and thus the assumption of uniform and instantaneous heating is sound. This is supported by the measurement of the Ti-K α emission from the rear surface of the sample (see Fig. 4), showing a smooth intensity distribution of the line emission across the transverse direction.

In order to compare with previously published data, we use the dimensionless parameter λ that is related to the coupling coefficient by $g = 3\lambda\hbar C_e \langle \omega^2 \rangle / \pi k_B T_e$, where $\langle \omega^2 \rangle \approx T_D^2/2$ [48]. This gives $\lambda \sim 0.03$, a value that is considerably closer to room temperature graphite [26,27] ($\lambda \lesssim 0.2$) than to values reported for metals and plasmas. However, our result is almost an order of magnitude less, suggesting the relaxation pathway is inhibited by the highly nonequilibrium conditions. Near room temperature, lower λ values in semimetals are attributed to a small density of states at the Fermi energy, an argument that does not hold here due to the high electron temperatures ($T_e \sim 10\,000$ K). This suggests a more complex energy pathway in warm dense graphite which acts as a barrier to relaxation.

Our present results are in good agreement with the energy relaxation time scale inferred from experiments where the graphite was heated by proton beams instead of fast electrons [16]. There a coupling constant of $g = 0.54 \times 10^{16} \text{ W K}^{-1} \text{ m}^{-3}$ was found. This suggests that the energy equilibration is independent of the details of the heating mechanism.

There is still much debate over energy relaxation in highly nonequilibrium materials particularly when related to the formation of WDM states. The experimental difficulties in creating these states and measuring ion temperatures within dense matter systems means that only a few data points exist. Previous experiments performed on warm

dense silicon and aluminum samples also suggest a very low coupling parameter [13,15] of the order of $10^{16} \text{ W K}^{-1} \text{ m}^{-3}$. Such processes may thus be characteristic of all warm dense matter states.

To explain these experimental results, it was proposed that the effective electron-ion interaction is suppressed by virtue of a dynamical coupling of electron and ion modes [20–22,49]. This experiment conclusively shows the need for improved models for energy relaxation in this warm dense regime, either through theoretical models involving coupled ion modes or numerical modeling such as Monte Carlo or particle-in-cell simulations. Moreover, we can expect that such low equilibration times in dense plasmas could lead to changes in other transport quantities, such as the optical conductivity and opacities, which may have a number of important implications ranging from the laser processing of materials and inertial confinement fusion [19] to the cooling rates of white dwarf stars and neutron stars [3,7].

The authors acknowledge the expert support of the staff at the PHELIX laser facility at GSI, Darmstadt, and the use of computing resources provided by STFCs e-Science facility. This work was partially supported by LaserLAB Europe and by AWE PLC.

*thomas.white@physics.ox.ac.uk

†g.gregori1@physics.ox.ac.uk

- [1] S. E. Bouffelfel, A. R. Oganov, and S. Leoni, *Sci. Rep.* **2**, 471 (2012).
- [2] A. Pelka *et al.*, *Phys. Rev. Lett.* **105**, 265701 (2010).
- [3] S. Ichimaru, *Rev. Mod. Phys.* **54**, 1017 (1982).
- [4] T. Guillot, *Science* **286**, 72 (1999).
- [5] E. Garcia Saiz *et al.*, *Nat. Phys.* **4**, 940 (2008).
- [6] A. L. Kritcher *et al.*, *Science* **322**, 69 (2008).
- [7] J. Daligault and S. Gupta, *Astrophys. J.* **703**, 994 (2009).
- [8] M. K. Matzen, M. A. Sweeney, R. G. Adams, and J. R. Asay, *Phys. Plasmas* **12**, 055503 (2005).
- [9] S. H. Glenzer *et al.*, *Science* **327**, 1228 (2010).
- [10] J. E. Bailey, G. A. Rochau, R. C. Mancini, C. A. Iglesias, J. J. MacFarlane, I. E. Golovkin, C. Blancard, Ph. Cosse, and G. Faussurier, *Phys. Plasmas* **16**, 058101 (2009).
- [11] B. A. Remington, R. P. Drake, and D. D. Ryutov, *Rev. Mod. Phys.* **78**, 755 (2006).
- [12] H. E. Elsayed-Ali and T. Juhasz, *Phys. Rev. B* **47**, 13599 (1993).
- [13] P. Celliers, A. Ng, G. Xu, and A. Forsman, *Phys. Rev. Lett.* **68**, 2305 (1992).
- [14] A. Ng, P. Celliers, G. Xu, and A. Forsman, *Phys. Rev. E* **52**, 4299 (1995).
- [15] D. Riley, N. C. Woolsey, D. McSherry, I. Weaver, A. Djaoui, and E. Nardi, *Phys. Rev. Lett.* **84**, 1704 (2000).
- [16] T. G. White *et al.*, *Sci. Rep.* **2**, 889 (2012).
- [17] L. Spitzer, *Physics of Fully Ionized Gases* (Interscience, New York, 1962).
- [18] H. Brysk, *Plasma Phys.* **16**, 927 (1974).
- [19] A. Ng, *Int. J. Quantum Chem.* **112**, 150 (2012).

- [20] G. Gregori and D. O. Gericke, *Europhys. Lett.* **83**, 15 002 (2008).
- [21] M. W. C. Dharma-wardana and F. Perrot, *Phys. Rev. E* **58**, 3705 (1998).
- [22] D. A. Chapman, J. Vorberger, and D. O. Gericke, *Phys. Rev. E* **88**, 013102 (2013).
- [23] S. Y. Zhou, G.-H. Gweon, J. Graf, A. V. Fedorov, C. D. Spataru, R. D. Diehl, Y. Kopelevich, D.-H. Lee, S. G. Louie, and A. Lanzara, *Nat. Phys.* **2**, 595 (2006).
- [24] S. Schäfer, W. Liang, and A. H. Zewail, *New J. Phys.* **13**, 063030 (2011).
- [25] A. M. Lindenberg *et al.*, *Science* **308**, 392 (2005).
- [26] Y. Ishida, T. Togashi, K. Yamamoto, M. Tanaka, T. Taniuchi, T. Kiss, M. Nakajima, T. Suemoto, and S. Shin, *Sci. Rep.* **1**, 64 (2011).
- [27] C. Leem *et al.*, *Phys. Rev. Lett.* **100**, 016802 (2008).
- [28] J. D. Lee, S. W. Han, and J. Inoue, *Phys. Rev. Lett.* **100**, 216801 (2008).
- [29] K. Sugawara, T. Sato, S. Souma, T. Takahashi, and H. Suematsu, *Phys. Rev. Lett.* **98**, 036801 (2007).
- [30] S. Piscanec, M. Lazzeri, F. Mauri, A. C. Ferrari, and J. Robertson, *Phys. Rev. Lett.* **93**, 185503 (2004).
- [31] H. Yan, D. Song, K. Fai Mak, I. Chatzakis, J. Maultzsch, and T. F. Heinz, *Phys. Rev. B* **80**, 121403 (2009).
- [32] M. Scheuch, T. Kampfrath, M. Wolf, K. von Volkman, C. Frischkorn, and L. Perfetti, *Appl. Phys. Lett.* **99**, 211908 (2011).
- [33] S. C. Wilks, A. B. Langdon, T. E. Cowan, M. Roth, M. Singh, S. Hatchett, M. H. Key, D. Pennington, A. MacKinnon, and R. A. Snavely, *Phys. Plasmas* **8**, 542 (2001).
- [34] U. Zastra *et al.*, *Phys. Rev. E* **81**, 026406 (2010).
- [35] T. Missalla, I. Uschmann, E. Förster, G. Jenke, and D. von der Linde, *Rev. Sci. Instrum.* **70**, 1288 (1999).
- [36] T. G. White *et al.*, CLF Annual Report 2012/2013 High Power Laser Science—Theory and Computation, 2013.
- [37] J. S. Green *et al.*, *Phys. Rev. Lett.* **100**, 015003 (2008).
- [38] M. Coury *et al.*, *Phys. Plasmas* **20**, 043104 (2013).
- [39] A. M. Lindenberg, *Science* **308**, 392 (2005).
- [40] See Supplemental Material at <http://link.aps.org/supplemental/10.1103/PhysRevLett.112.145005> for detailed descriptions of the fast electron density, current, electric and magnetic fields, and resistivity as predicted by the hybrid transport code ZEPHYROS.
- [41] S. Kar, A. P. L. Robinson, D. C. Carroll, O. Lundh, K. Markey, P. McKenna, P. Norreys, and M. Zepf, *Phys. Rev. Lett.* **102**, 055001 (2009).
- [42] S. Ichimaru, *Statistical Plasma Physics* (Westview Press, Boulder, CO, 2004), Vol. II.
- [43] H. O. Pierson, *Handbook of Carbon, Graphite, Diamond, and Fullerenes: Properties, Processing, and Applications* (Noyes Publications, New Jersey, 1993).
- [44] C. Klein, *Rev. Mod. Phys.* **34**, 56 (1962).
- [45] A. G. R. Thomas, M. Sherlock, C. Kuranz, C. P. Ridgers, and R. P. Drake, *New J. Phys.* **15**, 015017 (2013).
- [46] K. J. Peterson, D. B. Sinars, E. P. Yu, M. C. Herrmann, M. E. Cuneo, S. A. Slutz, I. C. Smith, B. W. Atherton, M. D. Knudson, and C. Nakhleh, *Phys. Plasmas* **19**, 092701 (2012).
- [47] K. J. Peterson, D. B. Sinars, E. P. Yu, M. C. Herrmann, M. E. Cuneo, S. A. Slutz, I. C. Smith, B. W. Atherton, M. D. Knudson, and C. Nakhleh, *Phys. Plasmas* **20**, 056305 (2013).
- [48] S. D. Brorson, A. Kazeroonian, J. S. Mooder, D. W. Face, T. K. Cheng, E. P. Ippen, M. S. Dresselhaus, and G. Dresselhaus, *Phys. Rev. Lett.* **64**, 2172 (1990).
- [49] J. Vorberger, D. O. Gericke, Th. Bornath, and M. Schlanges, *Phys. Rev. E* **81**, 046404 (2010).